

Absorption Spectra of a Graphene Embedded One Dimensional Fibonacci Aperiodic Structure

Hadi Rahimi^{*,1}

¹ Department of Physics, Islamic Azad University, Shabestar Branch, Shabestar, Iran

(Received 13 Sep. 2018; Revised 10 Oct. 2018; Accepted 28 Nov. 2018; Published 15 Dec. 2018)

Abstract: In this paper, we explore the linear response of one dimensional quasiperiodic structure based on Fibonacci sequence composed of silicon dioxide, polystyrene and graphene materials. Here, a graphene monolayer is sandwiched between two adjacent layers. The numerical results are obtained by using the standard transfer matrix method. Due to the presence of graphene sheet in each structure, in the initial range of THz, an additional gap GPBG is induced which is absent in the case of without graphene. The amplitude of absorption peaks at the upper edge of the GPBG significantly enhances, when damping factor increases. The height of the absorption peak at the GPBG edge goes up as the temperature increases. At the GPBG edge, with increasing the thickness of graphene, the absorption peak rises and shifts to the lower frequencies. Moreover, we have realized that the amplitude of absorption peaks at the upper edge of the GPBG significantly enhance by increasing damping factor.

Keywords: Graphene, Spectroscopy, Band gap, Quasiperiodic structures.

1. INTRODUCTION

Periodic structures have inherent potentials that have been subject of important theoretical developments in both solid state physics and photonics engineering. Photonic crystals (PCs) are structures that have periodic refractive-index modulation, long-range translational order and rotational point symmetry. Analogous to electrons in a crystal, electromagnetic waves propagating in PCs are organized into photonic bands that are separated by gaps where propagating states are forbidden [1-4].

On the other hand, the physical properties of a new class of artificial crystal, the so-called quasiperiodic structures, have also attracted a lot of attention in the last two decades. These quasicrystals are formed by the superposition of two (or more) incommensurate periods, so that they can be defined as intermediate

* Corresponding author. Email: h_rahimi@tabrizu.ac.ir

systems between a periodic crystal and the random amorphous solids. Photonic Quasicrystals may exhibit PBG that are more isotropic than in conventional photonic crystals, permitting the existence of forbidden frequency ranges even in materials possessing very low dielectric contrast. Among the various quasiperiodic structures, the Fibonacci binary quasiperiodic structure has been the subject of extensive efforts in the last two decades [5]. Macia used transfer matrix method (TMM) to study Fibonacci dielectric multilayers, numerically [6]. Omni-directional band gaps, using Fibonacci quasiperiodic structures, were also reported by Lusk. [7]. Peng have observed resonant transmission of light in symmetric Fibonacci multilayers, characterized by many perfect transmission peaks, useful for narrow band multi-wavelength optical filtering applications [8]. Studies of some other various aspects of wave propagation in the Fibonacci quasiperiodic structures carried out in refs. [9] have considerably improved our understanding of wave transport in the Fibonacci structures.

Recently, PCs composed of graphene and dielectric materials have started to attract research interest [10-14]. As a type of gapless semiconductor, graphene consists of two-dimensional (2D) honeycomb lattice with monolayer of carbon atom thickness, and was widely used in physics, chemistry, materials science and other fields [15]. Because of a variety of peculiar optical, mechanical and electronic properties like having zero band gap, high mobility at normal temperature, tunable conductivity and special optical properties, graphene attracts more attention in optoelectronic devices such as ultra fast optical modulator [16], graphene photodetectors [17], tunable optical sensor [18], graphene metamaterials [19], graphene plasmonics [20], terahertz absorber [21].

In this paper, by using the standard transfer matrix method (TMM), we explore the linear response of a 1D QP structure based on Fibonacci sequence composed of silicon dioxide (SiO_2), polystyrene and graphene materials. Here, a graphene monolayer is sandwiched between the two adjacent layers.

2. THEORETICAL MODEL

In this paper, we take a certain level of 1D Fibonacci quasiperiodic structure to calculate the transmission spectra of this deterministic disorder multilayer. The Fibonacci sequence is the chief example of long-range order without periodicity [18], and can be constructed from juxtaposing two building blocks A and B, according to the following deterministic generation rule: $S_{N+1} = \{S_{N-1}S_N\}$ for $N \geq 1$, with $S_0 = \{B\}$ and $S_1 = \{A\}$, and the generation rule is repeatedly applied to obtain: $S_2 = \{AB\}$, $S_3 = \{ABA\}$, $S_4 = \{ABAAB\}$, etc. This structure can be also generated by the following inflation rule: $A \rightarrow AB$, $B \rightarrow AA$. The number of layers is given by F_N , where F_N is the Fibonacci number obtained from recursive relation $F_N = F_{N-1} + F_{N-2}$, with $F_0 = F_1 = 1$.

The transmission spectra of a layered system can be calculated by using transfer matrix method. For this purpose, we assume that a wave be incident from air with angle θ onto the supposed multilayer structure. For the transverse electric (TE) wave, the electric field E is assumed in the x direction (the dielectric layers are in the x - y plane), and the z direction is normal to the interface of each layer. When such an electromagnetic wave propagates through this multilayer structure, the incident, reflected and transmitted electric fields are connected via a transfer matrix M [1-4] as

$$M_j(\Delta z, \omega) = \begin{pmatrix} \cos(k_z^j \Delta z) & j/q_j \sin(k_z^j \Delta z) \\ jq_j \sin(k_z^j \Delta z) & \cos(k_z^j \Delta z) \end{pmatrix} \quad (1)$$

Where $k_z^j = (\omega/c) \sqrt{\varepsilon_j} \sqrt{\mu_j} \sqrt{1 - \sin^2/\varepsilon_j \mu_j}$ is the component of the wave vector along the z axis, c indicates the speed of light in vacuum, $q_j = \sqrt{\varepsilon_j} / \sqrt{\mu_j} \sqrt{1 - \sin^2/\varepsilon_j \mu_j}$ for TE polarization, and $j = A, B$. The transmission coefficient can be expressed as

$$t(\omega, \theta) = \frac{2 \cos \theta}{(m_{11} + m_{22}) \cos \theta + i(m_{12} \cos^2 \theta - m_{21})} \quad (2)$$

Here $m_{ij}(i, j=1; 2)$ are the matrix elements of $X_N(\omega) = \prod_{j=1}^N M_j(d_j, \omega)$ which represents the total transfer matrix connecting the fields at the incidence and exit ends. The treatment for TM wave is similar to that for TE wave.

Graphene is a one-atom-thick layer of carbon atoms arranged in a two dimensional hexagonal lattice, which has recently attracted enormous interest for its abundant potential applications. The relative permittivity of graphene is given by $\varepsilon_g = 1 + (i\sigma_g \eta_0) / (k_0 d_g)$, where $k_0 = 2\pi/\lambda$ is the incidence wave number in vacuum, $\eta_0 = 377\Omega$ is the vacuum impedance, σ_g is the surface conductivity and λ is the incident wavelength. According to the Kubo formula [22], surface conductivity σ_g of graphene is obtained by intraband and interband terms as

$$\sigma_g = \sigma_{intra} + \sigma_{inter} \quad (3)$$

$$\sigma_{intra} = \frac{ie^2 k_B T}{\pi \hbar^2} \frac{1}{\omega + i\gamma} \left(\frac{\mu_c}{k_B T} + 2 \ln[1 + \exp(-\frac{\mu_c}{k_B T})] \right) \quad (4)$$

$$\sigma_{inter} = i \frac{e^2}{4\pi \hbar^2} \ln \left[\frac{2|\mu_c| - \hbar(\omega + i\gamma)}{2|\mu_c| + \hbar(\omega + i\gamma)} \right] \quad (5)$$

Where e is the charge of electron, $\hbar = h/2\pi$ is the reduced Plank's constant, k_B is the Boltzmann constant, T (300K) is the absolute temperature of environment, $\gamma = 1/\tau$ is the damping constant, τ is the transport relaxation time and μ_c is the

chemical potential. Despite, the intraband conductivity is larger than the interband in the THz band; here both terms are taken into account for the calculation of the surface conductivity. The intraband term of the conductivity is a reasonable approximation in the frequency range below 8 THz [22].

3. RESULTS AND DISCUSSION

Here, we present some numerical results to illustrate the transmission and absorption spectra of 1D Fibonacci QP structure with generation F8 (with 34 slabs). The supposed structures are constituted by SiO_2 (layer A) and polystyrene (layer B) dielectrics where graphene monolayer (layer G) is located between two adjacent layers. For this study, all layers are assumed to be linear, homogenous and nonmagnetic. The diagrams of supposed multilayers are presented in Fig. 1. The permittivity, permeability and the thickness of layers of A and B are as follows: $\epsilon_A=5$ [23], $\epsilon_B=2.5$ [24], $\mu_A=\mu_B=1$, $d_A=d_B=10\mu\text{m}$. Also, the values of chemical potential, damping constant and temperature of graphene sheet are assumed to be $\mu_c=0.2\text{eV}$, $\gamma=0$ and $T=300\text{K}$, respectively. Our numerical results are presented in the THz region.

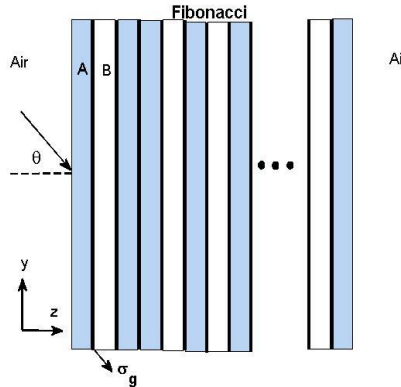


Fig. 1. Diagram of the supposed 1D Fibonacci quasiperiodic multilayer.

Firstly, by using Eqs. (4) and (5), the normalized surface conductivity σ/σ_0 of graphene as function of frequency is depicted in Fig. 2 for $\gamma = 0$ and (see Fig. 2a) and $\gamma=1 \text{ THz}$ (see Fig. 2b). Here, we use $\mu_c=0.2\text{eV}$ and $T=300\text{K}$. The σ_0 is the universal conductance of graphene.

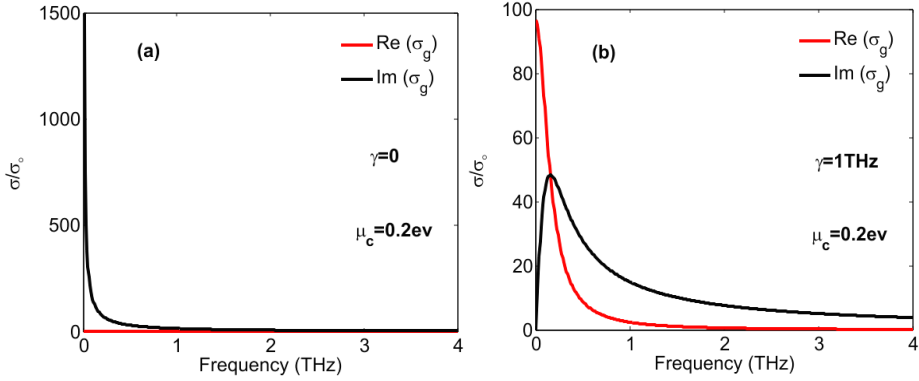


Fig. 2. Normalized surface conductivity σ/σ_0 of graphene as function of frequency for $\gamma=0$ (a) and $\gamma=1\text{THz}$ (b). We set $\mu_c=0.2\text{eV}$ and $T=300\text{K}$. σ_0 is the universal conductance of graphene sheet. Solid lines are for the real parts dashed lines are for the imaginary parts.

From Fig. 2, the imaginary (solid line) and real (dashed line) parts depend on the frequency, μ_c and γ . For a certain frequency, the conductivity of graphene increases with the increase of μ_c . As a result, the impact of graphene on the propagation characteristics of wave through the stack will be enhanced. For a certain μ_c , when the frequency increases the conductivity of graphene decreases quickly. About γ which is related to the absorption loss, we can say that the higher γ is, the larger the real part of the conductivity and then stronger the absorption, vice versa. In $\gamma=0$, the real part of the conductivity compared to the imaginary part is very negligible (see Fig. 1a). Also, in the case of $\gamma \neq 0$ the real part of conductivity increases while the imaginary part decreases (see Fig. 2b).

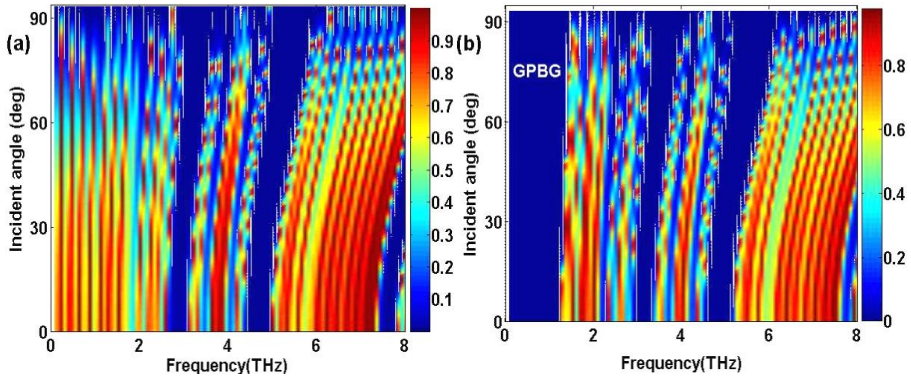


Fig. 3. TE transmission spectra of F_8 structure as function of frequency and incident angle. (a) without graphene, (b) with graphene. Here, for graphene layer, we set $T=300\text{K}$, $\gamma=0$ and $\mu_c=0.2\text{eV}$. The other parameters are the same as those in Fig. 1.

The spectral analysis in this section begins with the investigation of the transmission spectra in the supposed F_8 structure as a function of incident angle and frequency in the linear regime associated with TE mode in two situations: (i) without graphene, (ii) with graphene. It is seen from Fig. 3b that due to the presence of graphene sheet inside each structure, in the initial range of THz, an additional perfect gap is induced in the transmission spectra which is absent in the case of without graphene (see Fig. 3a). So, the first gap can be called graphene photonic band gap (GPBG). In addition to the GPBG, between 2 to 6 THz, some Bragg gaps are observed in the transmission spectra which are sensitive to the incident angle, frequency, structure parameters and polarization. For all selected structures, it is illustrated in Fig. 3 that when the incident angle varies, the upper and lower band edges of Bragg gaps experience a blue shift (tilt to the right) in accordance with the Bragg-Snell law. The transmission spectra of F_8 are simple and well-set. The similar figures can be presented for TM mode.

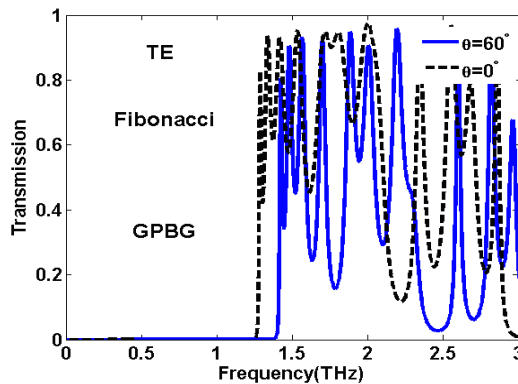


Fig. 4. 2D line plot of TE transmission spectra (same as Fig. 3b) at two incident angles as 0° (dashed line) and 60° (solid line). The other parameters are kept constants as in Fig. 3.

In order to gain deeper insight into the GPBG, we focus on the first PBG in the transmission spectra nearly below 1.5 THz for TE wave. In Fig. 4, two angles of incidence 0° (dashed line) and 60° (solid line) are selected. The other parameters are kept constants as in Fig. 3. In F_8 arrangement, it is found that moving away from normal incidence to oblique incidence shows that the upper band edge of the GPBG shifts to higher frequencies. That is to say, by increasing the incident angle the bandwidth ($\Delta\nu$) of the GPBG is obviously enlarged.

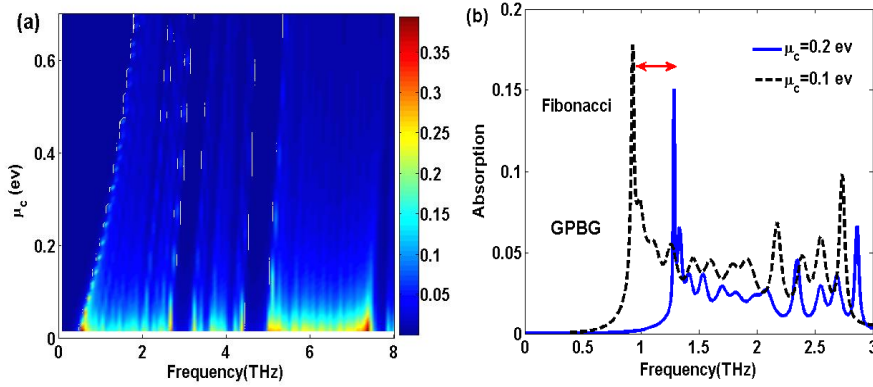


Fig. 5. TE absorption spectra of F_8 structure as a function of frequency and μ_c for $T=300\text{K}$ and $\gamma=0$. (a) X-Y view of 3D illustration, (b) 2D line plot at two chemical potentials as $\mu_c=0.1\text{eV}$ (dashed line) and $\mu_c=0.2\text{eV}$ (solid line). The other parameters are the same as those in Fig. 1.

Then, at normal incident angle and $\gamma=0$, we turn to study the absorption spectra of F_8 structure as a function of frequency and chemical potential μ_c . It is noticed that the amount of frequency dependent absorption is determined according to $A(\nu)=1-T(\nu)-R(\nu)$ where $T(\nu)$ and $R(\nu)$ denote the transmittance and reflectance at frequency ν , respectively. According to Fig. 5a, one can conclude that as μ_c increases the upper band edge of the GPBG moves to the higher frequencies, i.e., the GPBG becomes larger. The reason for this treatment is that for a certain frequency, the conductivity of graphene σ_g increases with the increase of μ_c , thus the impact of graphene on the propagation characteristics of wave will be enhanced. Meanwhile, the band edges and widths of the Bragg gap are slightly affected by changing of μ_c , since the conductivity of graphene changes more slowly in the high-frequency range (see Fig. 2). In Fig. 5b, which is a 2D line plot of Fig. 5a, two chemical potential are assumed as $\mu_c=0.1\text{eV}$ (dashed line) and $\mu_c=0.2\text{eV}$ (solid line). From Fig. 5b, it is found that the percentage of absorption peak at the edge of the GPBG lies within the range of about 16-18% for F_8 structure. The similar results can be found for TM mode.

In the above calculations, we have considered an idealized situation in which the role of damping factor γ , related to the absorption loss, has been neglected. As we know, the higher the γ is, the larger the real part of σ_g and then the stronger the absorption, vice versa. It is worth remembering that in the frequency ranges 0-10 THz, the losses of A and B layers can be neglected. In Fig. 6a, we show the TE absorption spectra of F_8 arrangement versus frequency and γ at normal incident angle.

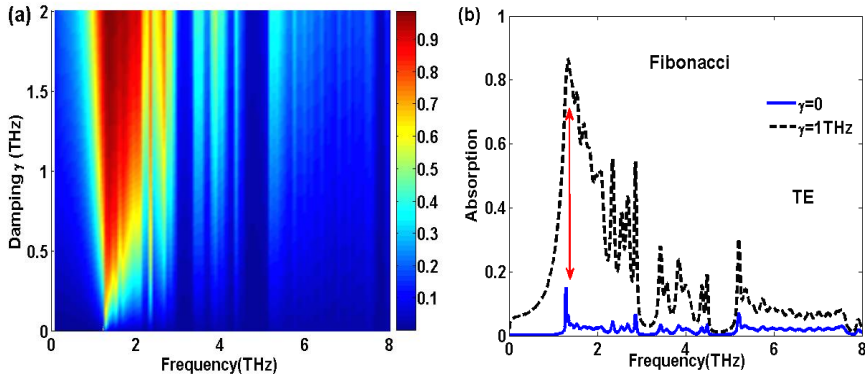


Fig. 6. TE absorption spectra of F_8 structure as a function of frequency and damping factor γ for $T=300\text{K}$ and $\mu_c=0.2\text{eV}$. (a) X-Y view of 3D illustration, (b) 2D line plot at $\gamma=0$ (dashed line) and $\gamma=1\text{THz}$ (solid line).

It can be seen from Fig. 6a that with the increase of γ , the GPBG in all structures will disappear gradually. Also, the spectral positions of the Bragg gaps remain unchanged. In the form of 2D line-plot, the effect of damping factor on the absorption peak at the edge of the GPBG is clearly demonstrated for $\gamma=0$ (solid line) and $\gamma=1\text{THz}$ (dashed line), shown in Fig. 6b. From this figure, we realize that the amplitude of absorption peaks at the upper edge of the GPBG significantly enhance by increasing γ .

As it is clear from Eqs. 4 and 5, the conductivity of graphene depends not only on frequency, μ_c and γ but also on temperature. Here, μ_c and γ are fixed at 0.2eV and 0, respectively. In Fig. 7, at room temperature $T=300\text{K}$ (solid line) and $T=310\text{K}$ (dashed line), the effect of the temperature on the TE absorption spectra of chosen structure is plotted at normal incidence. It is found that the absorption spectra of F_8 structure are approximately insensitive to the working temperature. Despite this slight and poor effect, we can say that the height of the absorption peak at the upper edge of the GPBG goes up as the temperature increases (see inset in Fig. 7). The similar results are obtained for TM wave.

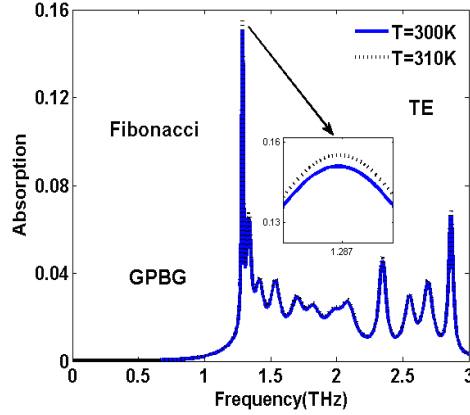


Fig. 7. 2D line plot of TE absorption spectra of F_8 structure at two temperatures $T=300\text{K}$ (solid line) and $T=310\text{K}$ (dashed line) for $\mu_c=0.2\text{eV}$ and $\gamma=0$. The other parameters are the same as those in Fig. 1.

In Sect. 2. 4, it was said that the permittivity of graphene layer is expressed in terms of the conductivity as $\epsilon_g=1+(i\sigma_g)/(\omega\epsilon_0d_g)$, where the d_g is the thickness of graphene layer. Various groups have reported different thicknesses for single layer graphene with ranging from 0.35 to 1.7 nm [25]. With this in mind, in Fig. 8, we simulate the influence of two supposed graphene thickness as $d_g=1\text{nm}$ (solid line) and $d_g=100\text{nm}$ (dashed line) on the TE absorption spectra at normal incident angle. As shown in Fig. 8, in each structure the upper band edge of GPBG, which we focus on, is minor affected by d_g . As a matter of fact, due to the very thin thickness of monolayer graphene (about 1nm), the absorption effect can be limited. Nevertheless, by carefully looking at the insets of Fig. 8, at the upper band edge of the GPBG two results obtain with increasing d_g as: (i) the absorption peak is downward to the lower frequencies, (ii) the height of the absorption peak rises. The similar behavior is repeated for TM mode.

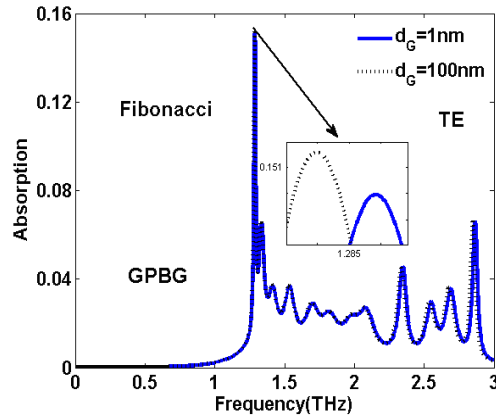


Fig. 8. 2D line plot of TE absorption spectra of F_8 structure at two graphene thickness as $d_g=1nm$ (solid line) and $d_g=100nm$ (dashed line) for $\mu_c=0.2ev$, $\gamma=0$ and $T=300K$. The other parameters are the same as those in Fig. 1.

Finally, in order to know how the electromagnetic wave propagates in F_8 1D multilayer, at the edge frequency (f_{edge}) and inside frequency (f_{inside}) of the GPBG, the distribution of electric field intensity as a function of structure depth (z) is plotted at normal incident angle (see Fig. 9). The electric field intensity is calculated by the TMM knowing the parameters of structure and solving Maxwell equations with the boundary conditions appropriate. Here, the total thickness of all structures is about 0.3 mm. From all insets in Fig. 9, one can say that the electric field in each supposed structure are continuous at two side of the interface between two adjacent layers. At the band edge frequencies the mode is propagating, while at the frequencies inside the gap the mode is evanescent, i.e., the electromagnetic waves are completely reflected by structure.

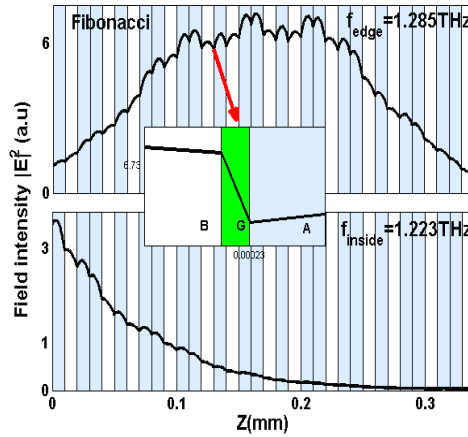


Fig. 9. The electric field intensity profile (the square of electric field) as a function of structure depth (z) in F_8 multilayer at the edge frequency (f_{edge}) and inside frequency (f_{inside}) of the GPBG for normal incident angle. Again, we choose $\mu_c=0.2ev$, $\gamma=0$, $T=300\text{K}$ and $d_g=1\text{nm}$. The other parameters are the same as those in Fig. 1.

4. CONCLUSION

By employing the transfer matrix method, we have reported the terahertz spectral properties of graphene induced photonic band gap in four types of common one-dimensional quasiperiodic structures based on Fibonacci sequence. In this paper, a graphene monolayer is sandwiched between two adjacent dielectric slabs. It is found that due to the presence of graphene in each structure, an additional gap (GPBG) is emerged. The upper band edge of GPBG moves to the higher frequencies and gets enlarged, as the chemical potential and incident angle increase. Also, the height of the absorption peak at the GPBG edge goes up as the temperature increases. At the GPBG edge, with increasing the thickness of graphene, the absorption peak rises and shifts to the lower frequencies. Moreover, we have realized that the amplitude of absorption peaks at the upper edge of the GPBG significantly enhance by increasing γ .

REFERENCES

- [1] Z. Zare and A. Gharaat. Investigation of thermal tunable nano metallic photonic crystal filter with mirror. JOPN. [Online]. 3 (3) (2018, Summer) 27-36. Available: http://jopn.miau.ac.ir/article_3043.html.
- [2] T. Froutan fard kobar olia1 and A. Vahedi. Temperature Tunability of Dielectric/ Liquid Crystal / Dielectric Photonic Crystal Structures. JOPN. [Online]. 2(4) (2017, Autumn) 57-70. Available: http://jopn.miau.ac.ir/article_2574.html.

- [3] R. Talebzadeh and M. Bavaghar. *Tunable Defect Mode in One-Dimensional Ternary Nanophotonic Crystal with Mirror Symmetry*. JOPN. [Online]. 2(4) (2017, Autumn) 83-92. Available: http://jopn.miau.ac.ir/article_2576.html.
- [4] K. Milanchian and Z. Eyni. Analytical Investigation of TM Surface Waves in 1D Photonic Crystals Capped by a Self-Focusing Left-Handed Slab. JOPN. [Online]. 2(4) (2017, Autumn) 19-32. Available: http://jopn.miau.ac.ir/article_2571.html.
- [5] N. Ansari and E. Mohebbi. *Broadband and high absorption in Fibonacci photonic crystal including MoS2 monolayer in the visible range*. J. Phys. D: Appl. Phys. [Online]. 51(11) (2018) 115342-115348. Available: <http://iopscience.iop.org/article/10.1088/1361-6463/aaacbd/meta>.
- [6] E. Macia. *Optical applications of Fibonacci dielectric multilayers*. Ferroelectrics. [Online]. 250 (2001, March) 401-410. Available: <https://www.tandfonline.com/doi/abs/10.1080/00150190108225111>.
- [7] D. Lusk. *Omnidirectional reflection from Fibonacci quasi-periodic one-dimensional photonic crystal*. Opt. Commun. [Online]. 198 (2001, November) 273-279. Available: <https://www.sciencedirect.com/science/article/abs/pii/S0030401801015310>.
- [8] R. W. Peng. *Symmetry-induced perfect transmission of light waves in quasiperiodic dielectric multilayers*. Appl. Phys. Lett. [Online]. 80 (2002, April) 3063. Available: <https://aip.scitation.org/doi/10.1063/1.1468895>.
- [9] H. Zhang, S. Liu, X. Kong, B. Bian and Y. Dai. *Omnidirectional photonic band gaps enlarged by Fibonacci quasi-periodic one-dimensional ternary superconductor photonic crystals*. Solid State Commun. [Online]. 152 (2012, December) 2113-2119. Available: <https://www.sciencedirect.com/science/article/pii/S0038109812005297>.
- [10] C. H. Costa, L. F. C. Pereira, and C. G. Bezerra. *Light propagation in quasiperiodic dielectric multilayers separated by graphene*. Phys. Rev. B. [Online]. 96 (2017, September) 125412. Available: <https://journals.aps.org/prb/abstract/10.1103/PhysRevB.96.125412>.
- [11] F. U. Al-sheqefi and W. Belhadj. *Photonic band gap characteristics of one-dimensional graphene-dielectric periodic structures*. Superlattices and Microstructures. [Online]. 88 (2015, December) 127-138. Available: <https://www.sciencedirect.com/science/article/pii/S0749603615301853?via%3Dihub>.

- [13] Y. Chen, L. Bian, P. Liu, G. Li, Y. Xie. *Controlling light absorption and transmission in graphene-embedded structure with Fano resonance and FP resonance*. Superlattices and Microstructures. 124 (2018, December) 185-191. Available: <https://www.sciencedirect.com/science/article/pii/S074960361831396X>.
- [14] Ali Moftakharzadeh, B. Afkhami Aghdaand Mehdi Hosseini. *Noise Equivalent Power Optimization of Graphene- Superconductor Optical Sensors in the Current Bias Mode*. JOPN. [Online]. 3 (3) (2018, Summer) 1-12. Available: http://jopn.miau.ac.ir/article_3040.html.
- [15] V. Singh, D. Joung, L. Zhai, S. Das, S. I. Khondaker and S. Seal, *Graphene based materials: Past, present and future*. Prog. Mater. Sci. [Online]. 56 (2011, October) 178-1271. Available: <https://www.sciencedirect.com/science/article/pii/S0079642511000442?via%3Dihub>.
- [16] Y. Yamaguchi, S. Takagi and M. Takenaka. *Low-loss graphene-based optical phase modulator operating at mid-infrared wavelength*. Jpn. J. Appl. Phys. [Online]. 57 4) (2018, March) 401-406. Available: <http://iopscience.iop.org/article/10.7567/JJAP.57.04FH06>.
- [17] S. Aydin, B. Kalkan, C. Varlikli and C. elebi, *P3HTgraphene bilayer electrode for Schottky junction photodetectors*. Nanotechnol. [Online]. 29 (14) (2018, February) 145502-145511. Available: <http://iopscience.iop.org/article/10.1088/1361-6528/aaaaf5/meta>.
- [18] Y. Li, L. Qi, J. Yu, Z. Chen, Y. Yao and X. Liu. *One-dimensional multi-band terahertz graphene photonic crystal filters*. Opt. Mater. Express. [Online]. 7 (2017, May) 1228-1239. Available: <https://www.osapublishing.org/ome/abstract.cfm?uri=ome-7-4-1228>.
- [19] D. Smirnova. *Deeply subwavelength electromagnetic Tamm states in graphene metamaterials*. Phys. Rev. B. [Online]. 89 (2014, June) 245414. Available: <https://journals.aps.org/prb/abstract/10.1103/PhysRevB.89.245414>.
- [20] B. Zhao and Z. M. Zhang. *Strong Plasmonic Coupling between Graphene Ribbon Array and Metal Gratings*. ACS Photonics. [Online]. 2 (11) (2015, October) 1611-1618. Available: <https://pubs.acs.org/doi/abs/10.1021/acsphotonics.5b00410>.
- [21] A. Andryieuski and A. V. Lavrinenko. *Graphene metamaterials based tunable terahertz absorber: effective surface conductivity approach*. Opt. Express. [Online]. 21 (2013, April) 91449155. Available: <https://www.osapublishing.org/oe/abstract.cfm?uri=oe-21-7-9144>.

- [22] L. Falkovsky and S. Pershoguba. *Optical far-infrared properties of a graphene monolayer and multilayer*. Phys. Rev. B. [Online]. 76 (15) (2007, October) 153410. Available: <https://journals.aps.org/prb/abstract/10.1103/PhysRevB.76.153410>.
- [23] H. Hung, C. Wu and S. Chang. *Terahertz temperature-dependent defect mode in a semiconductor-dielectric photonic crystal*. J. Appl. Phys. [Online]. 110 (2011, October) 093110. Available: <https://aip.scitation.org/doi/abs/10.1063/1.3660230>.
- [24] J. Topham, O. Boorman, I. L. Hosier, M. Praeger, R. Torah, A. Vaughan, T. Andritsch and S. G. Swingler. *Dielectric studies of polystyrene-based, high-permittivity composite systems*. IEEE. [Online]. (CEIDP) (2014, October) 711-714. Available: <https://ieeexplore.ieee.org/document/6995854>.
- [25] C. Shearer, A. D. Slattery and A. J. Stapleton. *Accurate thickness measurement of graphene*, Nanotechnol. [Online]. 27 (2016, February) 125704. Available: <http://iopscience.iop.org/article/10.1088/0957-4484/27/12/125704/pdf>.